

# 4-D RECONSTRUCTION OF THE LEFT VENTRICLE FROM A SINGLE CYCLE ULTRASOUND ACQUISITION

Claudia Bonciu<sup>1,\*</sup>, Rodolphe Weber<sup>1</sup>, Long Dang Nguyen<sup>2</sup>

1.Laboratoire d'Electronique, Signaux, Images. Université d'Orléans  
BP 6744, 45067 Orléans cédex 2, France

Tel: +33 2 38494562 ; fax: +33 2 38417245 ; e-mail: clbonciu@tuiasi.ro

2.Centre Hospitalier Régional d'Orléans 45100 Orléans La source, France

## ABSTRACT

A new acquisition system using a fast rotating 2-D ultrasound probe is proposed to reconstruct the deformations of the left cardiac ventricle. During only one cardiac cycle, the high resolution probe acquires successive conic sections of the left ventricle. Then, assuming that the contours have been accurately detected, the set of sparse spatio-temporal data, which correspond to the successive intersection points of the moving ultrasound beam with the endocardiac wall, is spatially and temporally interpolated to estimate the continuous variation of the volume. This reconstruction is achieved through an iterative algorithm based on the harmonic 4-D model of the volume considered as a periodic multidimensional signal [1]. Results are clinically promising.

## 1 INTRODUCTION

In cardiology, 3-D or 4-D measurements, particularly applied to the left ventricle (LV), are of prime interest to characterize the cardiac function [4] [5] [9] [8]. To perform such spatio-temporal measurements, ultrasound imaging is a fast, non-invasive and low-cost alternative compared to other imaging techniques.

In this paper, a 4D acquisition system using a *fast continuously* rotating 2-D ultrasound probe is presented. During the ultrasound beam scanning, the probe rotation is not stopped. Its speed can reach 8.7 revolutions per second at an acquisition rate of 48 images per second. With these high rates, the spatio-temporal sampling of the LV is high enough to limit the acquisition time to *a single cardiac cycle* (typically 0.7 second). Moreover, unwanted motions of both the operator and the patient occurring during the acquisition time are no more significant. Thus, related artifacts and distortions generated during the reconstruction phase are neglected. Besides, by avoiding the need to average several successive cardiac cycles, new clinical investigations become possible. For example, this system would be well adapted to detect segmental hypoki-

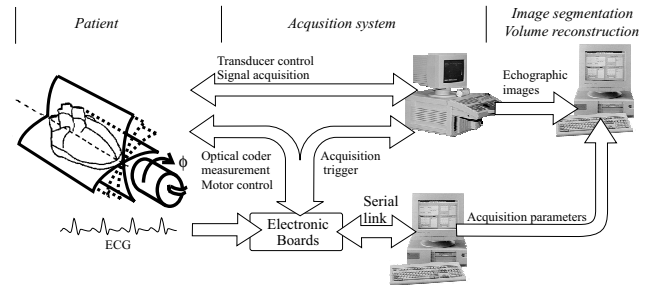


Figure 1: Schematic view of the complete processing line of our 4D LV reconstruction system.

nesia in stress test ultrasound and in accurate studies of systolic function during arrhythmia. The acquisition system architecture and the geometry of the resulting cross sections are described in Section 2. Considering that the LV contours have been accurately detected, reconstruction is achieved through an iterative algorithm based on the harmonic 4-D model (H4DM) of the volume considered as a periodic multidimensional signal. This point is addressed in Section 3. Section 4 describes some clinical results. Some concluding remarks and a discussion on further work end the paper.

## 2 SYSTEM DESCRIPTION

Fig. 1 shows the overall block diagram for the experimental 4D echographic imaging system. A commercial 2D real-time ultrasound scanner (ESAOTE AU4) drives a very fast rotating probe which makes continuous apical cross sections of the LV. The first computer is in charge of both the interactive segmentation of images and the reconstruction of the LV. The second one drives specific electronic boards. An electrocardiogram (ECG) acquisition system provides additional information for image labelling.

### 2.1 Probe description

The 2D rotating probe (see Fig. 2) has a cylindrical shape and is composed of two main parts : the ultrasonic transducer array and the motor. The ultrasonic transducer array is a conventional 64 elements phased

\*on leave for Technical University "Gh. Asachi" of IASI, Electrical Engineering Faculty, Departement of Power Systems, Bd. D. Maneron 51-53 IASI-6600-ROMANIA.

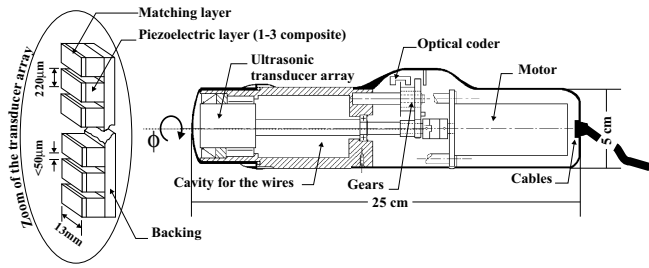


Figure 2: Schematic view of the rotating probe and details of the 64-elements ultrasound transducer array. With appropriate positioning of the wires in the cavity, the transducer can be rotated  $720^\circ$ .  $\phi$  is the rotation angle.

array. Its dimensions are given in Fig. 2. This sensor rotates around its central axis. Rotation is controlled by a direct current motor. Due to the electrical connection between the array and the front-end electronics, the maximum rotation angle is limited to 720 degrees from the initial position; beyond this critical angle the cables would be damaged. An optical coder measures the rotation angle,  $\phi$ , of the sensor each 7.11 ms with a high accuracy (0.18 degrees). This information is used to place data in the spatio-temporal co-ordinates.

## 2.2 Characteristic of the scanning

Generally, 3D ultrasound imaging systems acquire successive plane slices. In such a system, acquisition is not performed during the step-by-step motion of the transducer. Instead, the system must wait until the movement stops to perform the acquisition. This is not a major disadvantage when static rigid objects are explored, but becomes a significant drawback in the deformable objects case. In our approach, a continuous motor has been preferred to a stepper motor in order to increase the number of images acquired during one cycle. However, owing to the combination of the different motions (rotation and scanning), our acquired images are no longer plane slices of the LV but conic slices (see Fig. 3.a). In practice, the rotation speed may differ slightly from its nominal value and measurements from the optical coder are used to reconstruct the exact shape of the slice. Top view of Fig. 3.b shows an example of successive scan positions. At the end of the scanning operation, the beam is reset to its initial position relative to the transducer. The use of an electronic phase array means that this reset time can be neglected and acquisition is considered as being continuous.

## 2.3 Characteristics of the processed data

In the present development phase, endocardial contours are traced manually. In the next phase, only several systolic and diastolic contours will be drawn. These contours will be used as initial conditions for an automatic extraction method based on the harmonic active model

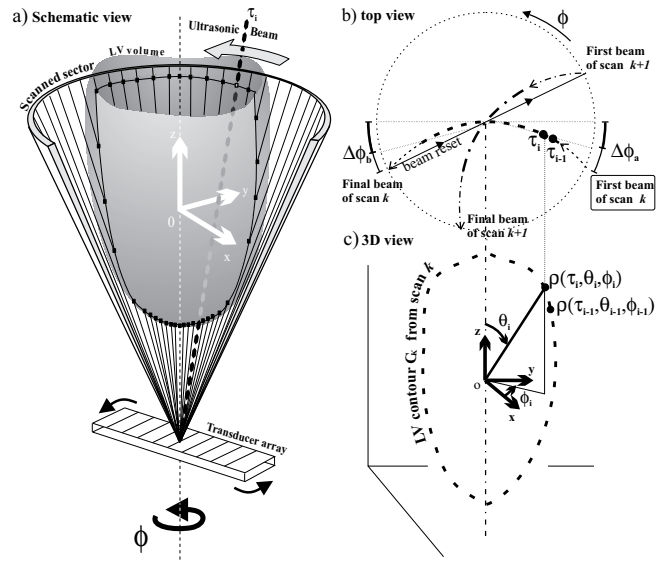


Figure 3: (a) Schematic view of the scanning shape. The combination of the transducer rotation and the linear beam sweep generates a conic slice. A temporal indexation,  $\tau_i$ , is done on the successive beams. The origin of the co-ordinates,  $O$ , is chosen along the rotation axis. (b) Schematic top view of 3 successive scans. At the end of a scan, the reset time is neglected. (c) Each scan is segmented and contours of the LV volume are extracted. Temporal indexing is carried out on these successive intersection points of the moving ultrasound beam with the endocardial wall. Thus, acquired data are in the form,  $\{\rho_i\} = \{\rho(\theta_i, \phi_i, \tau_i)\}_{i=1, \dots, N}$ , where  $\rho_i$ ,  $\theta_i$ ,  $\phi_i$  are spherical co-ordinates and  $\tau_i$  is the time normalized on the cardiac cycle duration.

(HAM) [1].

After segmentation, knowing the probe rotation law and the scanning beam movement law, each point of each contour,  $C_k$ , can be placed in a global spatial coordinate system. Moreover, as electronic scanning is not instantaneous, temporal labelling is performed for each beam and, consequently on each point of each contour. Let us denote this instant of acquisition,  $\tau_i$ , (see Fig. 3).

Thus, initial data are assumed to be spatio-temporal samples belonging to the exact LV hyper-surface. These data are placed in a spherical and temporal co-ordinate system. The spatial origin,  $O$ , is chosen inside the left ventricle along the rotation axis of the probe (see Fig. 3.a). Let us denote,  $\rho(\theta, \phi, \tau)$ , the LV hyper-surface and,  $\{\rho_i\} = \{\rho(\theta_i, \phi_i, \tau_i)\}_{i=1, \dots, N}$ , the set of initial data, where  $\theta, \theta_i \in [0, \pi]$ ,  $\phi, \phi_i \in [0, 2\pi]$ ,  $\tau, \tau_i \in [0, 1]$  and  $N$  is the number of initial data extracted from the contours.

Due to the sequential characteristic of the acquisition device, the initial data,  $\{\rho_i\}$ , are sparse and irregularly spaced. The objective is now to retrieve the missing data. This point is addressed in the following section.

### 3 4-D reconstruction

Different approaches can be used to reconstruct the temporal evolution of the LV volume [2], [3], [6], [10], [11]. In this paper, a new technique of dynamic volume reconstruction is proposed. It is based on spatio-temporal harmonic modeling applied on  $\rho(\theta, \phi, \tau)$ . An iterative interpolation is done to restore the missing data. The iterative procedure is related to an algorithm proposed by Papoulis for band-limited extrapolation [7].

From  $\rho(\theta, \phi, \tau)$ , which is intrinsically periodic in  $\phi \in [0, 2\pi]$  and in  $\tau \in [0, 1]$ , another set of data  $\bar{\rho}(\theta, \phi, \tau)$ , which is in addition periodic in  $\theta \in [0, \pi] \cup [\pi, 2\pi]$  is considered by means of:

$$\begin{cases} \bar{\rho}(\theta, \phi, \tau) = \rho(\theta, \phi, \tau) & \text{if } \theta \in ]0, \pi[ \\ \bar{\rho}(\theta, \phi, \tau) = \rho(2\pi - \theta, \phi + \pi, \tau) & \text{if } \theta \in ]\pi, 2\pi[ \\ \bar{\rho}(0, \phi, \tau) = \text{constant} & \forall \phi \\ \bar{\rho}(\pi, \phi, \tau) = \text{constant} & \forall \phi \end{cases}$$

The problem now is to restore, from the set of measured sparse data  $\{\rho_i\}$ , all the missing points of the tri-periodic hyper-surface  $\bar{\rho}(\theta, \phi, \tau)$ . This is done by an iterative algorithm based on the 3D Fourier transform of a discrete version of  $\bar{\rho}(\theta, \phi, \tau)$ .

The iterative algorithm used in this study consists of the following steps :

1. the hyper-surface,  $\bar{\rho}$ , is initialized by the set of measured data  $\{\rho_i\}$ . The missing data of the hyper-surface are initialized by data derive from an average radius.
2. a discrete 3-D Fourier transform is applied on  $\bar{\rho}$ .
3. a low pass filtering is applied, forcing to zero all the Fourier coefficients which are out of a given ellipsoid. The cut-off frequencies depend on the acquisition configuration.
4. a discrete 3-D inverse Fourier transform yields a new estimation of the surface,  $\bar{\rho}$ . At this step, the estimated surface does not match the set of initial data.
5. an error criterion is computed between the estimated surface and the set of initial data, which are supposed to belong to the true surface. If this error is above a given threshold, the set of measured data,  $\{\rho_i\}$ , are placed back into the data set corresponding to the last estimation of the volume,  $\bar{\rho}$ , and the algorithm loops back to the second step. Otherwise, the iterative procedure is stopped.

In fact, the resulting hyper-surface converges to a spatio-temporal interpolation of the initial set of sparse data, coherent with the imposed frequency constraint. From this 3-D algorithm, 2-D and 1-D algorithms are derived. They are used respectively to reconstruct LV volume from consecutive contours belonging to a given temporal window and to model the contours.

### 4 Experimental results

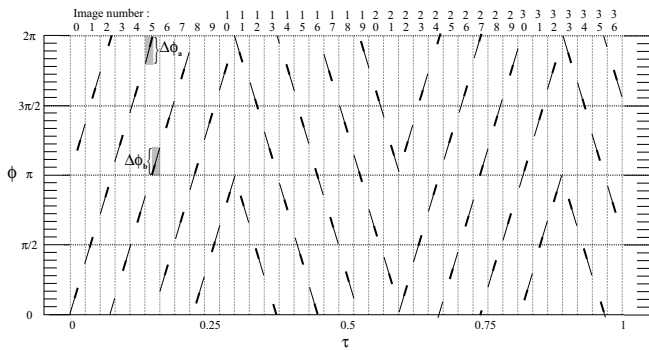


Figure 4: Projection of the 3-D data grid upon  $\phi$  ( $0^\circ \leq \phi \leq 2\pi$ ) and  $\tau$  ( $0 \leq \tau \leq 1$ ). Each dash highlights the angular sector scanned during the acquisition of half an image. For example the angular sectors of image number 5,  $\Delta\phi_a$  and  $\Delta\phi_b$ , are drawn on Fig 3.b. Bold dashes indicate the most probable position of contours.

In order to assess the effectiveness of the reconstruction procedure described above, clinical experiments were carried out in the cardiology department of the Regional Hospital in Orléans (France). The configuration of the system is described in Fig. 1. The system is used to store over 100 consecutive digital images,  $508 \times 508$  pixels, 8 bit per pixel depth. The rotation speed was approximately 8.7 revolutions per second and the acquisition rate was 48 images per second. The patient has a pacemaker and his cardiac cycle duration was 768 ms so that approximately 37 images were acquired during one cycle.

The probe rotation angle during one scan,  $\Delta\phi$ , was theoretically  $65.25^\circ$ . Given that one complete rotation is not a multiple of  $\Delta\phi$ , a progressive shift of the position of the scanned sectors is done. This yields a good angular coverage of the LV and improves the spatial accuracy of the rendered volumes. In Fig. 4, these angular sectors are plotted over the normalized cardiac cycle.

After segmentation, approximately  $N = 3000$  measurement points,  $\{\rho_i\}$ , of a single cardiac cycle were available. The reconstruction algorithm was applied to a grid sampling in  $\theta, \phi, \tau$ , which was respectively  $64 \times 64 \times 64$ . Fig. 5 shows examples of reconstruction at different moments in the cardiac cycle. The ejection fraction,  $F_{ej}$ , has been estimated from our measurements of the end-systolic and end-diastolic volumes ( $F_{ej} = 0.416$ ). The classical estimation of  $F_{ej}$  shows results in good agreement with our estimation. This value corresponds to hypokinesia of the ventricular wall, resulting from a coronary thrombosis, as the other clinical investigations have shown.

### 5 Conclusions

This paper has presented the preliminary results of reconstructing the LV in four dimension, using ultrasound

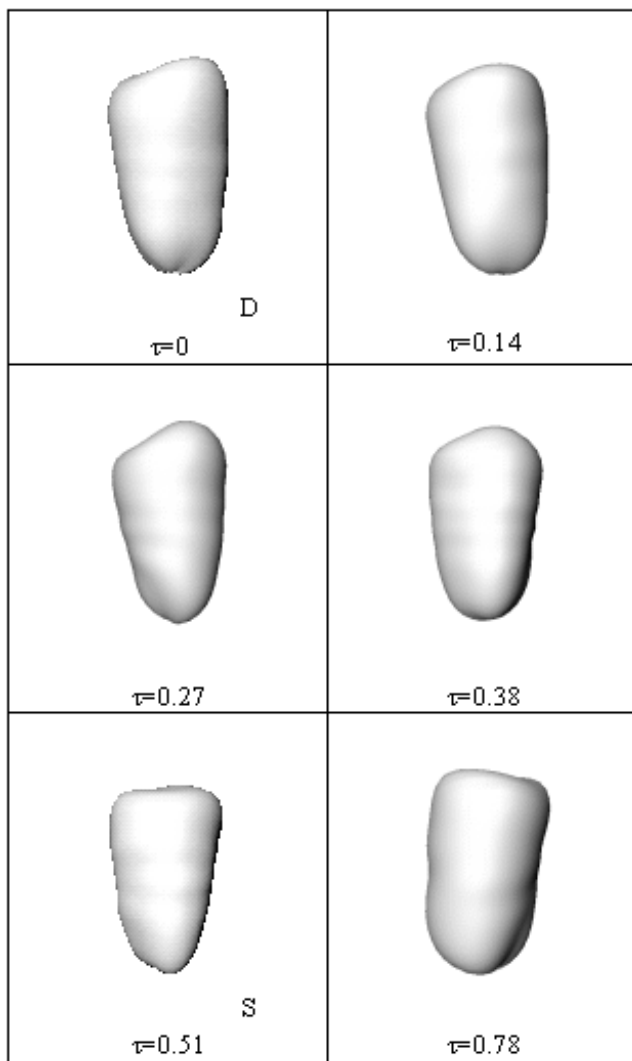


Figure 5: Examples of the 64 reconstructed LV volumes.  $\tau$  is the normalized time. **D** (respectively **S**) represents the end-diastolic (resp. end-systolic) volume.

data acquired during only one cardiac cycle. A new trans-thoracic probe has been developed for this purpose. This probe is specially designed for high-frequency acquisition systems, and does not require a recovery time, unlike step-by-step movement probes. Consequently, the probe may be used to acquire data on deformable objects, thus providing a better limit on the spectral distribution of the spatio-temporal data points. A specific harmonic modeling technique was developed to cope with the geometrical complexity of the reconstruction problem, which produces an uniform but sparse data distribution in the reconstruction space. Preliminary clinical results are promising and comparisons with other 4-D techniques are planned. Technical studies on the improvement of the spatio-temporal sampling and computer studies on the improvement of the algorithm are under investigation.

**Acknowledgments :** The authors wish to thank the ANVAR (Agence Nationale de Valorisation de la Recherche) for its involvement and financial support for this research project.

## References

- [1] Cl. Bonciu (1997) *4D Reconstruction of the left ventricle using echographic images*, PhD thesis, Université d'Orléans, France.
- [2] Cl. Bonciu, S. Treuillet, W. Ohley (1998) *Reconstructing periodic evolving ellipsoid from 2D slices by a signal processing approach*, Congrès RFIA'98, Clermont-Ferrand, France, 91-100.
- [3] G. Coppini, R. Poli, G. Valli (1995) *Recovery of The 3D Shape of Left Ventricle from Echocardiographic Images*, IEEE Transactions on Medical Imaging, 14, 2, 301-317.
- [4] A. Fenster, D. Downey (1996) *3-D Ultrasound Imaging : A review*, IEEE Engineering in Medicine and Biology, 15, 6, 41-51.
- [5] J. Greenleaf, M. Belohlavek, T. Gerber, D. Foley, J. Seward (1993) *Multidimensional Visualization in Echocardiography : An Introduction*, Mayo Clin Proc, 68 : 213-220.
- [6] A. Matheny and D. Goldgof (1995) *The use of three- and four-dimensional surface harmonics for rigid and nonrigid shape recovery and representation*, IEEE Trans. on Pattern Analysis and Machine Intelligence, 17, 10, 967-981.
- [7] A. Papoulis (1975) *A New Algorithm in Spectral Analysis and Band-Limited Extrapolation*, IEEE Trans. on Circuits and Systems, 22, 9, 735-742.
- [8] A. Salustri and J. R. Roelandt (1995) *Ultrasonic three-dimensional reconstruction of the heart* Ultrasound in Medicine and Biology, 21, 3, 281-293.
- [9] J. B Seward, M. Belohlavek, P. W. O'Leary, D. A. Foley, and J. F. Greenleaf (1995) *Congenital heart disease: wide-field, three-dimensional, and four-dimensional ultrasound imaging* American Journal of Cardiac Imaging, 9, 1, 38-43.
- [10] L. Staib and J. Duncan (1992) *Deformable Fourier models for surface finding in 3-D images*, Visualization in Biomedical Computing, SPIE, 1808, 90-104.
- [11] D. Terzopoulos and D. Metaxas (1991) *Dynamic 3D models with local and global deformations: deformable superquadrics*, IEEE Trans. on Pattern Analysis and Machine Intelligence, 13, 703-714.